

# Laser-induced fluorescence and thermoluminescence response of a Na–Ca rich silicate

V. Correcher<sup>a,\*</sup>, J. Garcia-Guinea<sup>b</sup>, M. Castillejo<sup>c</sup>, M. Oujja<sup>c</sup>, E. Rebollar<sup>c</sup>, P. Lopez-Arce<sup>d</sup>

<sup>a</sup>CIEMAT, Av. Complutense 22, Ed 2, Madrid 28040, Spain

<sup>b</sup>Museo Nacional de Ciencias Naturales (CSIC), C/Jose Gutierrez Abascal 2, Madrid 28006, Spain

<sup>c</sup>Instituto de Química Física Rocasolano CSIC, Serrano 119, Madrid 28006, Spain

<sup>d</sup>The Getty Conservation Institute, 1200 Getty Center Drive, Suite 700, Los Angeles, CA 90049, USA

Received 9 August 2005; received in revised form 7 April 2006; accepted 22 May 2006

## Abstract

Pectolite ( $\text{NaCa}_2\text{Si}_3\text{O}_8(\text{OH})$ ) is an inosilicate of hydrothermal origin hosted in Cretaceous basalt with calcite and iron oxides and is almost always associated with zeolites. The emission of this silicate was studied by laser-induced fluorescence (LIF) and thermal stimulated luminescence (TL). The fluorescence spectra of different areas of the sample induced by exposition to 266 nm UV laser light (5 nm of spectral resolution, FWHM) give rise to two peaks at 550 and 830 nm that can be, respectively, linked to the presence of  $\text{Mn}^{2+}$  and  $\text{Cr}^{3+}$  emission centres. The stability tests at different temperatures show clearly that the TL glow curves at 400 nm in natural pectolite samples, track the typical pattern of a system produced by a continuous trap distribution, well defined in other silicates. This process could be mainly associated to dehydroxylation effect, as observed by differential thermal analysis (DTA), and probably is also linked to chromophore oxidation. © 2006 Elsevier Ltd. All rights reserved.

**Keywords:** Laser-induced fluorescence; Thermoluminescence; Electron microprobe analysis; Differential thermal analysis

## 1. Introduction

Blue pectolite ( $\text{NaCa}_2\text{Si}_3\text{O}_8(\text{OH})$ ) or Larimar is an inosilicate of hydrothermal origin hosted in Cretaceous basalt with calcite and iron oxides that has been hardly investigated from a spectroscopic point of view. To the best of our knowledge, research on the emission properties of pectolite employing thermoluminescence (TL) and laser-induced fluorescence (LIF or laser fluorometric) techniques have never been investigated before. Spectroscopy techniques are of great interest to provide information on mineral characterisation that will be useful in future to be applied, for example, to the field of dating or retrospective dosimetry. LIF is a technique that can be employed for the determination of soil-contamination (Pepper et al., 2002), uranium in silicate rock (Aly et al., 1988) and measurements of nitric oxide in biological tissues (Ye et al., 2004). It is based on the emission of molecules excited to higher energy levels after the absorption of electromagnetic radiation.

The wavelength of the emitted light represents, therefore, the energy difference between the ground state and the excited state that always has a longer wavelength than that of excitation stage due to an energy loss in the fluorescence process. The fluorescence properties of different minerals allow for the monitoring of the relative chemical composition of the bulk flow. The possibility to study these excited states allows us: (i) to determine the type of changes that take place in the outer electron shell on deeper lying states; it is interesting to compare solid state spectra where the outer electrons are involved in binding (Boivin and Scime, 2003) and (ii) to obtain information about the dissociation processes (Uma and Das, 1994). One of the most interesting aspects of fluorescence detection compared to absorption measurements is the greater sensitivity attainable because the fluorescence signal has a very low background. Likewise, TL is used as a tool in the fields of archaeological and geological dating and retrospective dosimetry and from a basic point of view supplies information, among others, on: (i) trapped charge recombination sites related to metastable defects inside the lattice (McKeever, 1985), (ii) phase transitions (Correcher et al., 2004a) or (iii) consecutive breaking and

\* Corresponding author. Tel.: +34 91 346 6322; fax: +34 91 346 6005.  
E-mail address: [v.correcher@ciemat.es](mailto:v.correcher@ciemat.es) (V. Correcher).

linking of bonds including redox reactions, dehydroxylation and dehydration processes (Correcher et al., 2004b). As is well-known, TL is based on the emission of light from a dielectric solid sample (insulator or semiconductor) when it is heated after being irradiated (naturally or accidentally) by some kind of radiation such as X-rays, gamma rays, beam of electrons, etc. (McKeever, 1985). During the analytical heating, the TL signal is registered by a photomultiplier tube and recorded as a function of temperature or wavelength as a TL glow curve.

The aim of this paper is focused on the study of LIF (in the range of 300–1200 nm) and UV-blue TL behaviour of a sample of pectolite. This research is supported by the chemical analysis of different dyed zones of this silicate using electron microprobe analysis (EMPA) and the thermal transformations (dehydration and dehydroxylation) of this mineral achieved by differential thermal analysis–thermogravimetry (DTA–TG) technique.

## 2. Experimental

Samples of pectolite were analysed by means of EMPA. The studies were performed in a Jeol Superprobe JXA-8900M, with bulk and channel-selected (TAP, PETJ, LIF, PETH) X-ray spectra search and identification routines. Natural standards and synthetic crystals from the collection of the “Servicio de Microscopía Electrónica Luis Bru”, Complutense University, Madrid, have been used.

The sample ( $25 \times 25 \times 2 \text{ mm}^3$ ) displayed four coloured areas: brown, intense blue, white–blue and pure white. LIF spectra were collected in each of these four coloured zones of the sample and the measurements were carried out by illuminating the sample with the unfocused output of the fourth harmonic of a Nd:YAG laser at 266 nm (Quantel, Brilliant B, pulse width 5 ns, repetition rate 10 Hz). The laser beam was directed to the surface of the sample with the use of quartz prisms at  $45^\circ$  incidence to the surface of the sample (Castillejo et al., 2002). The beam spot at the surface had a diameter of 0.75 mm and the energy per pulse was around 0.1 mJ, resulting in a fluence of  $22 \text{ mJ cm}^{-2}$ . The fluorescence emitted from the surface of the sample was collected at right angles with respect to the laser beam direction and imaged onto the entrance slit of a 0.30 m spectrograph (TMC300 Bentham, 1200 grooves/mm, 500 nm blaze). Fluorescence spectra were recorded with a time gated ICCD camera (2151 Andor Technologies) placed at the spectrograph exit slit. The spectra were recorded, in intervals of 70 nm, in the 300–1200 nm wavelength range, with a resolution of 5 nm. The light emitted upon irradiation with each laser pulse was collected within in a temporal gate of 1 ms, at zero delay with respect to the laser pulse.

DTA–TG of  $50 \pm 2 \text{ mg}$  of sample was recorded with a simultaneous TG–DTA–DSC thermal analyser (Setaram, Labsys CS 32-CS 332 Controller) in air. Thermal treatments were performed at a heating rate of  $5^\circ \text{C min}^{-1}$  from ambient to  $1000^\circ \text{C}$ . The sample was in an alumina crucible and the reference material was alumina.

The thermal stability of the TL emission of pectolite was studied by testing the response following different sample

pre-heating treatments (from 250 to  $340^\circ \text{C}$ ). TL measurements were carried out using an automated Risø TL system model TL DA-12 (Bøtter-Jensen and Duller, 1992), this reader is provided with an EMI 9635 QA photomultiplier and the emission was observed through a blue filter (type FIB002 Melles-Griot) where the wavelength is peaked at 320–480 nm (FWHM,  $80 \pm 16 \text{ nm}$  with minimum peak of 60%). It is also provided with a  $^{90}\text{Sr}/^{90}\text{Y}$  source with a dose rate of  $0.020 \text{ Gy s}^{-1}$  calibrated against a  $^{60}\text{Co}$  photon source in a secondary standards laboratory (Correcher and Delgado, 1998). All the TL measurements were performed using a linear heating rate of  $5^\circ \text{C s}^{-1}$  from RT to  $550^\circ \text{C}$  in an atmosphere of nitrogen. Four aliquots of  $5.0 \pm 0.1 \text{ mg}$  each of pectolite were used for each measurement. The sample was carefully powdered with an agate pestle and mortar to avoid triboluminescence (Garcia-Guinea and Correcher, 2000). The incandescent background was subtracted from the TL data.

## 3. Results and discussion

### 3.1. Sample characterisation

The chemical characterisation of this silicate, performed under EMPA, displays the presence of  $\text{Cr}_2\text{O}_3$  0.42%;  $\text{TiO}_2$  1.59%,  $\text{MnO}$  0.32% and  $\text{Fe}_2\text{O}_3$  82.63% in the host rock (point 1 in Fig. 1 and Table 1). The analyse carried out on different dyed pectolite zones (points 2–11, Fig. 1 and Table 1), show different percentage of  $\text{Cr}_2\text{O}_3$  (up to 0.03%) and  $\text{V}_2\text{O}_5$  (up to 0.06%). The linkages among  $\text{FeOOH}:\text{Cr}$  with blue rings and the  $\text{V}_2\text{O}_5$  background in the pectolite masses (and not in  $\text{FeOOH}$ ) suggest hydrothermal remobilisation of basaltic chromite crystals and vanadium from a bottomless source in hydrothermal fluids. The anisotropic green colour can be attributed to the

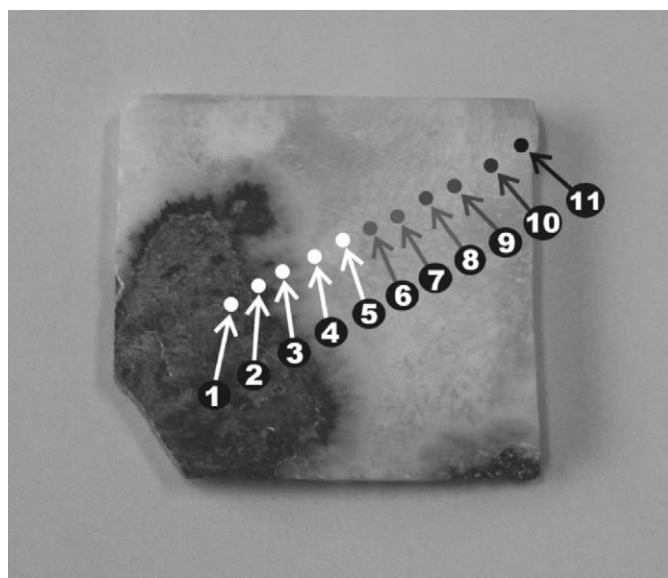


Fig. 1. Sample of blue pectolite ( $\text{NaCa}_2\text{Si}_3\text{O}_8(\text{OH})$ ) ( $25 \times 25 \times 2 \text{ mm}^3$ ) employed for electron microprobe analysis (EMPA) and LIF measurements. Points 1–11 correspond to the position where the chemical analysis were carried out.

Table 1

Chemical characterisation of pectolite employing electron microprobe analysis (EMPA) where the greyed columns correspond to the brown (1), intense blue (3), pure white (5) and white-bluish (9) area

Core element	Host rock										
	1	2	3	4	5	6	7	8	9	10	11
SiO <sub>2</sub>	1.016	52.751	47.727	51.795	52.506	53.262	52.778	52.651	52.375	60.710	60.426
Al <sub>2</sub> O <sub>3</sub>	0.643	0.169	0.946	0.239	0.180	0.079	0.014	0.017	0.161	24.219	26.131
MgO	0.648	0.008	0.811	0.038	0.006	—	0.042	0.013	—	—	0.001
CaO	0.507	34.219	32.953	34.195	34.258	34.152	34.566	34.339	34.396	5.741	5.600
TiO <sub>2</sub>	1.590	0.027	1.323	—	0.023	34.152	34.566	34.339	34.396	5.741	5.600
P <sub>2</sub> O <sub>5</sub>	—	0.043	0.006	0.038	—	—	—	—	0.041	—	—
Na <sub>2</sub> O	0.098	9.194	7.333	8.707	9.022	0.018	—	—	0.005	0.034	0.018
K <sub>2</sub> O	0.005	0.048	0.004	0.029	0.026	8.882	9.161	9.241	8.711	8.676	8.376
Cu	—	0.058	—	—	0.045	—	—	—	—	—	—
Mn	0.325	0.280	0.496	0.187	0.135	0.138	0.118	0.104	0.259	0.007	0.024
Fe	82.626	0.058	4.128	0.189	0.116	0.017	0.107	0.049	0.017	0.046	0.145
Ni	—	—	0.032	—	0.001	0.010	0.006	—	0.032	0.173	0.381
Cr	0.416	—	—	0.001	0.023	—	0.009	—	0.026	0.032	—
V	—	0.056	0.019	—	0.021	0.025	—	0.007	—	—	0.008
F	—	0.097	—	—	—	—	—	0.029	0.006	0.041	0.043
Cl	—	0.001	0.005	0.016	—	0.013	—	0.002	—	0.002	—
Total	87.874	96.968	95.782	95.430	96.362	96.607	96.828	96.440	96.102	99.664	101.139

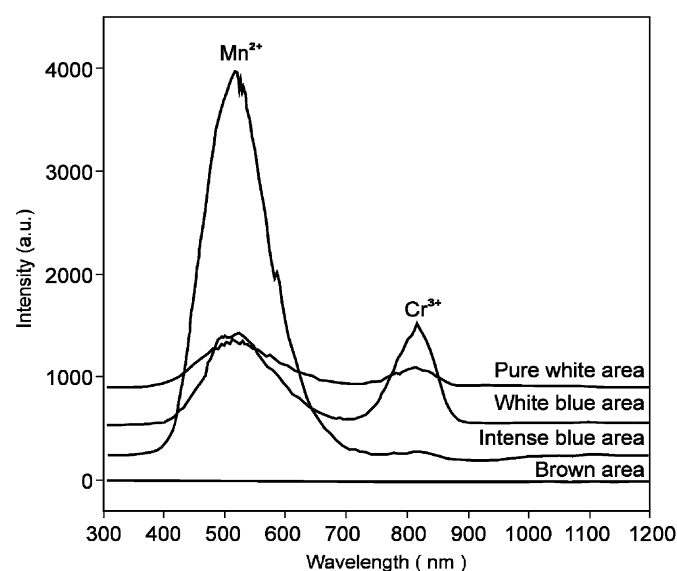


Fig. 2. Fluorescence spectra of different areas: (i) brown area (point 1), (ii) intense blue zone (points 2, 3 and 4), (iii) white–blue area (points 7, 9 and 10) and (iv) pure white area (points 5, 6, 8 and 11) of pectolite sample induced by 266 nm UV laser light. Spectral resolution is 5 nm.

different vanadium content, although a Ti<sup>4+</sup>–Fe<sup>2+</sup> intervalence-charge-transfer mechanism cannot be disregarded (i.e. TiO<sub>2</sub> from 0.02% to 1.3%).

### 3.2. LIF and TL emission

The four LIF spectra of different coloured areas of pectolite sample are shown in Fig. 2. The behaviour of the LIF emissions are characterised by the presence of two broad bands peaked at 510 and 810 nm where the fluorescence activators

for each emission were, respectively, assigned to Mn<sup>2+</sup> and Cr<sup>3+</sup> (Torchia et al., 2001). However, it is possible to appreciate changes in the ratio of the intensity of both emissions depending on the colour of the sample. Thus, both the intense blue (point 3) and the pure white (point 5) areas exhibit a more intense band due to the Mn<sup>2+</sup> content respect to the emission attributed to Cr<sup>3+</sup> ion (40:3 and 15:11, respectively). On the other hand, the proportion of the intensity of the fluorescence bands obtained for the white–blue (point 9) zone of this silicate is almost 1:1. The intensity of the fluorescence signal is proportional to the population of the species in the excited state, and the excited state population is proportional to the population of the initial state before the laser is turned on. The brown area of pectolite exhibits a flat fluorescence signal in the range of 300–1200 nm, probably due to the high content of Fe<sup>3+</sup> (82%) that could act as an inhibitor of the total emission. This suggests that in the iron rich area of pectolite, the photoexcitation at wavelengths shorter than 266 nm gives null fluorescence.

The UV-blue TL spectra of the white–blue sample (the brown area was excluded) was studied to determine the trap system of the components involved in the luminescent process. For this aim, progressive pre-annealed samples of pectolite ranging from a preheating temperature ( $T_{stop}$ ) of 250 up to 430 °C was performed, followed by quenching from the different temperatures to obtain aliquots with different grades of modulation of the lattice, thus determining the trap structure. As observed in Fig. 3, the TL glow curves of this inosilicate display a wide broad distribution, above 400 °C, in which it is possible to distinguish how the evolution of the whole TL curve shows a gradual and progressively linear shift of the maximum peak to higher temperatures and a change in the shape and intensity of the TL glow curve respect to the  $T_{stop}$ . This thermolabile broad

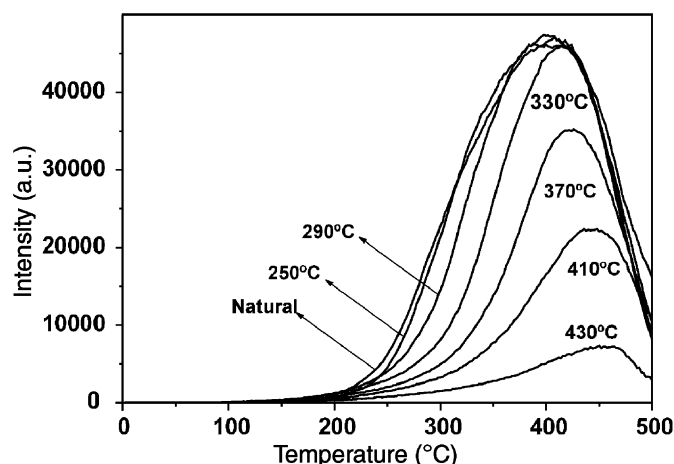


Fig. 3. Thermal stability of the natural TL emission of blue-white pectolite at different temperatures (250–430 °C).

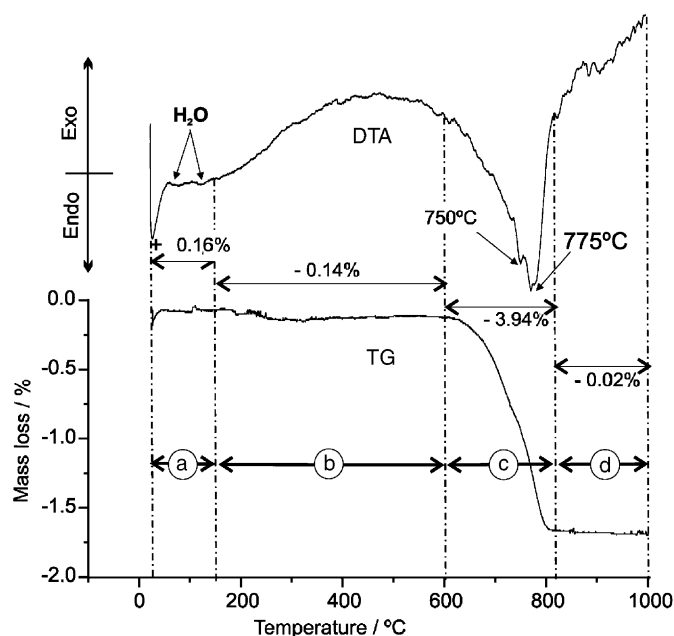


Fig. 4. DTA–TG of a pectolite sample obtained at a heating rate of  $50^{\circ}\text{C min}^{-1}$  from room temperature to  $1000^{\circ}\text{C}$ . The increase of the temperature induces changes in mass: (a) from room temperature to  $150^{\circ}\text{C}$  a gain of  $\sim 0.16\%$  associated with dehydration of adsorbed and absorbed water; (b) from  $150$  to  $600^{\circ}\text{C}$  a loss  $\sim 0.14\%$  due to no significant changes in the lattice structure; (c) from  $600$  to  $820^{\circ}\text{C}$  a loss of  $3.9\%$  caused by dehydroxylation process and (d) from  $820$  to  $1000^{\circ}\text{C}$  a loss of  $0.02\%$  linked to structural reorganisations of the dehydrated compound.

band of blue emissions shows TL glow curves of multi-order kinetics involving continuous processes of trapping–detraping or a continuum in the distribution of the traps. This behaviour has been also observed in other complex silicates (Garcia-Guinea et al., 2005) and feldspars (e.g. Na-rich feldspars; Correcher et al., 1999). During the thermal treatment in the TL measurement, the sample modifies the structure giving rise to different processes such as: dehydration, dehydroxylation, alkali-self diffusion, etc. The study of some of these processes has been

performed by means of DTA–TG technique. DTA is a sensitive method to determine endothermic and exothermic processes including: phase transitions, dehydration, and decomposition, redox, or solid-state reactions. It consists on the measurement of the difference in temperature between a sample and a reference as heat is applied to the system. On the other hand, TG is a useful technique for determining, among others, decomposition reactions; it is based on the measurement of the mass of a sample as the temperature increases. As observed in Fig. 4, the DTA curve of pectolite exhibits two small endothermic peaks from room temperature up to  $150^{\circ}\text{C}$ , at  $80$  and  $128^{\circ}\text{C}$ , due to dehydration of adsorbed and absorbed water, respectively. Beyond the latter temperature, the heat flow increases up to  $500^{\circ}\text{C}$ . At this point, it starts to decrease giving rise to a broad and sharp endothermic effect with a double peak at around  $750$  and  $775^{\circ}\text{C}$ . After this main endothermic reaction, produced in several steps and caused by dehydroxylation process, a serial of many endothermic and exothermic small peaks take place during the thermal analysis, beyond  $820^{\circ}\text{C}$  until  $1000^{\circ}\text{C}$ , due to structural reorganisations of the dehydrated compound. TG curve shows one gain and three mass losses due to the dehydration and dehydroxylation processes of pectolite. With increasing temperature, the following changes in mass occur: (Fig. 4a) from room temperature to  $150^{\circ}\text{C}$  a gain of  $\sim 0.16\%$ ; (Fig. 4b) from  $150$  to  $600^{\circ}\text{C}$  a loss  $\sim 0.14\%$ ; (Fig. 4c) from  $600$  to  $820^{\circ}\text{C}$  a loss of  $3.9\%$  and (Fig. 4d) from  $820$  to  $1000^{\circ}\text{C}$  a loss of  $0.02\%$ .

#### 4. Conclusions

The high sensitivity of LIF spectroscopy to characterise natural materials provides: (i) information about the electronic state of the luminescent species and (ii) the microenvironment surrounding these species. In this sense, the LIF technique provides information that supports a continuous trap distribution system since it should be considered as a consequence of many different processes (dehydration, dehydroxylation, alkali-self diffusion, etc.) due to the presence of non-homogeneous samples. The identification of luminescent emitters could help to understand some anomalous behaviour observed during the TL laboratory routine measurements. The fluorescence emission spectra of the blue-coloured zones of pectolite show the presence of two maxima peaked at  $510$  and  $810\text{ nm}$  that have been assigned, respectively, to  $\text{Mn}^{2+}$  and  $\text{Cr}^{3+}$ . This result is supported by the EMPA measurements where the linkages among  $\text{FeOOH}:\text{Cr}$  with blue rings and the  $\text{V}_2\text{O}_5$  background in the pectolite masses, and not in  $\text{FeOOH}$ , suggest hydrothermal remobilisation of basaltic chromite crystals and vanadium element from a bottomless source of the hydrothermal fluids. The thermal stability of the UV-blue luminescence emission demonstrates that the trap distribution is quite similar to other complex silicates (bavenite) and several feldspars, i.e. it should correspond to a continuous trap distribution. This behaviour could be associated to dehydration–dehydroxylation processes produced in the pectolite lattice since is well correlated with the DTA results.

## Acknowledgements

This work has been supported by CAM (06/0134/2003), MCYT (BQU2003-08531-C02-01); CICYT (CGL2004-03564/BTE) and Comunidad Autonoma de Madrid (CAM) MATERNAS-S-0505/MAT/0094 projects. Thanks are also given to Spanish Thematic Network on Cultural Heritage of CSIC for a fellowship (ER) and an I3P contract (MO).

## References

- Aly, M.M., Elalfy, M.S., Fattah, M.A., 1988. Determination of uranium in silicate rocks using laser-induced fluorescence. *J. Radioanal. Nucl. Ch.* 121 (1), 45–51.
- Boivin, R.F., Scime, E.E., 2003. Laser induced fluorescence in Ar and He plasmas with a tunable diode laser. *Rev. Sci. Instrum.* 74 (10), 4352–4360.
- Bøtter-Jensen, L., Duller, G.A.T., 1992. A new system for measuring OSL from quartz samples. *Nucl. Tracks Radiat. Meas.* 20, 549–553.
- Castillejo, M., Martín, M., Oujja, M., Silva, D., Torres, R., Manousaki, A., Zafropulos, V., van den Brink, O.F., Heeren, R.M.A., Teule, R., Silva, A., Gouveia, H., 2002. Analytical study of the chemical and physical changes induced by KrF laser cleaning of tempera paints. *Anal. Chem.* 74, 4662–4671.
- Correcher, V., Delgado, A., 1998. On the use of natural quartz as transfer dosimeter in retrospective dosimetry. *Radiat. Meas.* 29 (3–4), 411–414.
- Correcher, V., Gomez-Ros, J.M., Delgado, A., 1999. The use of albite as a dosimeter in accident dose reconstruction. *Radiat. Prot. Dosim.* 84 (1–4), 547–549.
- Correcher, V., Garcia-Guinea, J., Lopez-Arce, P., Gomez-Ros, J.M., 2004a. Luminescence emission spectra in the temperature range of the structural phase transitions of Na<sub>2</sub>SO<sub>4</sub>. *Spectrochim. Acta A* 60, 1431–1438.
- Correcher, V., Gomez-Ros, J.M., Garcia-Guinea, J., Delgado, A., 2004b. Thermoluminescence kinetic parameters of basaltic rock samples due to continuous trap distribution. *Nucl. Instrum. Methods A* 528, 717–720.
- Garcia-Guinea, J., Correcher, V., 2000. Luminescence spectra of alkali feldspars: influence of crushing on the ultraviolet emission band. *Spectrosc. Lett.* 33, 103–113.
- Garcia-Guinea, J., Correcher, V., Quejido, A., LaIglesia, A., Can, N., 2005. The role of rare earth elements and Mn<sup>2+</sup> point defects on the luminescence of bavenite. *Talanta* 65 (1), 54–61.
- McKeever, S.W.S., 1985. *Thermoluminescence of Solids*. Cambridge University Press, New York.
- Pepper, J.W., Wright, A.O., Kenny, J.E., 2002. In situ measurements of subsurface contaminants with a multi-channel laser-induced fluorescence system. *Spectrochim. Acta A* 58 (2), 317–331.
- Torchia, G.A., Muñoz, J.A., Cussó, F., Jaque, F., Tocho, J.O., 2001. The luminescent quantum efficiency of Cr<sup>3+</sup> ions in co-doped crystals of LiNbO<sub>3</sub>:ZnO determined by simultaneous multiple-wavelength photoacoustic and luminescence experiments. *J. Lumin.* 92, 317–322.
- Uma, S., Das, P.K., 1994. Dynamics of  $I^* (P - 2(1/2))$  production in the ultraviolet photodissociation of alkyl iodides. *Can. J. Chem.* 72 (3), 865–869.
- Ye, X.Y., Kim, W.S., Rubakhin, S.S., Sweedler, J.V., 2004. Measurement of nitric oxide by 4,5-diaminofluorescein without interferences. *Analyst* 129 (12), 1200–1205.